Optical Processing – 4F System

MATEO MORALES,[1] ESTEBAN VELÁSQUEZ,[1] MARÍA PAULA REY[1,*]

[1]*Physical Sciences Department, EAFIT University, Medellín, Colombia.*
**Corresponding author: mpreyb@eafit.edu.co*

Published 19 October 2021

The 4F system is a commonly used optical relay that consists of two lenses. The first lens performs a Fourier transform, and the second allows us to process the optical information of the transmittance by applying another Fourier transform of the frequency plane. Thus, these systems consist of a cascade of two Fourier transforms. In this work, we implemented a 4F optical imaging system and used it to perform optical processing operations on input transmittances by controlling the transmittance at the frequency plane of the system both experimentally and numerically, correctly obtaining the expected results according to the theory for each of the filters in both cases. © 2020 Optical Society of America

1. THEORETICAL BACKGROUND

The Fourier transform is an equivalent representation of a function or image (2D function) in terms of the weight of each frequency component that exists within the original function. A mathematical expression for the Fourier transform is [1]:

$$\Im\{f[x,y]\} = \Im[\zeta,\eta] = \int_{-\infty}^{+\infty}\int f[x,y]e^{-2\pi i(\zeta x+\eta y)}dxdy \quad (1)$$

This expression evaluates the set of projections of $f[x,y]$ onto each of the complex-valued sinusoids $e^{-2\pi i(\zeta x+\eta y)}$. The transform is a 2D array of data where the constant part (DC component) of $f[x,y]$ maps to $\Im[0,0]$ and the oscillating parts of $f[x,y]$ to other frequencies in $\Im$. The complex-valued spectrum $\Im[\zeta,\eta]$ may be represented as its real and imaginary parts or as its magnitude and phase:

$$\Im[\zeta,\eta] = Re\big[\Im[\zeta,\eta]\big] + i\,Im\big[\Im[\zeta,\eta]\big] = |\Im[\zeta,\eta]|e^{+i\phi\{\Im[\zeta,\eta]\}} \quad (2)$$

In (2), the propagation distance z_1 satisfies the condition $z_1 \gg \frac{x^2+y^2}{\lambda_0}$. Since the propagation distance z_1 must be considerable, this is not a practical means to evaluate the Fourier transform of the input function $f[x,y]$, which is often difficult or even impossible to achieve in some applications. Thus, according to the Fourier transforming properties of a lens, by adding a positive lens after the input function, we can produce the Fourier transforming system shown in Fig. 1.

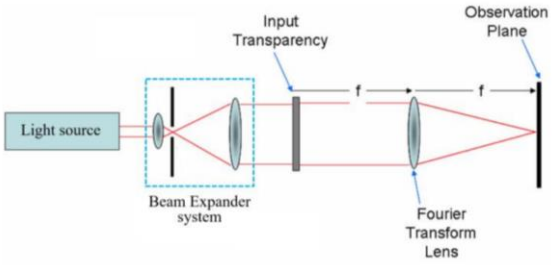

Fig. 1. Simple system for viewing the Fourier transform of an input transparency [1].

To process the optical information of a given transmittance, another Fourier transform operation is needed. The simplest way to do this is shown in Figure 2. If we add a second lens to compute the Fourier transform of the Fourier transform, we will have access to the frequency space of the input data. The second lens is located one focal length away from the Fourier transform plane, and the output is observed one focal length away from the lens. This setup is called a 4F imaging system [1].

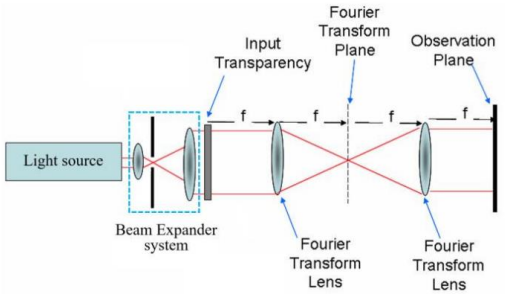

Fig. 2. System proposed in this laboratory experience [1].

It is easy to trace a ray from an arrow located at the object plane parallel to the axis to predict the behavior at the output plane of the imaging system. The image of this ray will be inverted, which indicates that the Fourier transform of the Fourier transform is a

reversed replica of the function $f[x, y]$, as theoretically expected. See equation (3) [1].

$$\Im_2\{\Im_2\{f[x,y]\}\} = \Im_2\left\{\Im\left[\frac{x}{\lambda_0 f}, \frac{y}{\lambda_0 f}\right]\right\} \backsim f[-x,-y] \qquad (3)$$

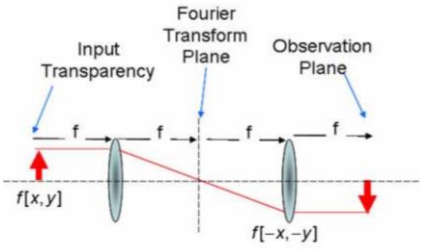

Fig. 3. Simple ray trace to predict that the output of the 4f-system is reversed [1].

This imaging system makes the Fourier transform $\Im[\zeta, \eta]$ of the input function $f[x, y]$ accessible in the Fourier transform plane or frequency plane [1].

2. METHODOLOGY

A. Element parameters

1. Coherent light source: B&W Tek BWT-20E/54168 Laser aperture
Wavelength: 532nm.

2. High energy pinhole:
Diameter aperture of 10 µm ± 1 µm [2].

3. Newport 10X Microscope objective.
Focal Length: 16.50mm
Numerical aperture: 0.25.
Working distance: 10.6mm [3].

5. Thorlabs AC254-200-A Tube Lens, Ø1" Achromatic Doublet.
AR Coating range: 400 - 700 nm.
Focal length = 200 mm [4].

6. Thorlabs DCC1645-HQ Imaging Source CMOS Camera
Pixel size: 3.6 µm, Square.
Imaging area (horizontal x vertical): 4.61 mm x 3.69 mm [5].

B. System for viewing the Fourier transform of an input transparency

In order to see the optical Fourier transform of a given input transparency, the setup presented in figure 1 was carry out using a coherent light source compose by a HeNe laser and a beam expander system (BES) with the 10X microscope objective and the pinhole of 10 µm. Additionally, the Fourier transform lens used is a positive lens with focal length of 10 cm due to the size of the supports used [Fig. 4].

In this way, controlling the size of the image with an iris diaphragm and using 3 different transparencies, 3 experimental Fourier transforms were captured and were subsequently contrasted with the numerical result of the transparency fast Fourier transform using an image of the transparency in Python.

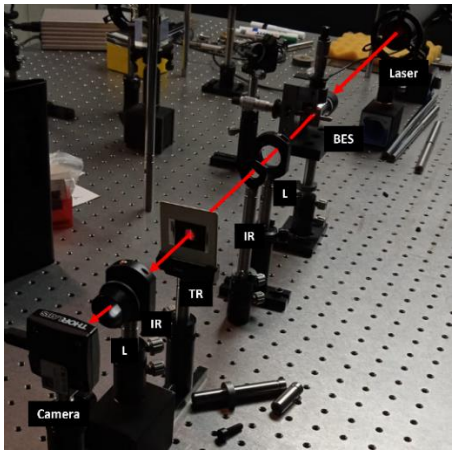

Fig. 4. 2F Optical Setup. L, lens; IR, iris; TR, transparency; BES, beam expander system.

C. 4F System

Subsequently, the 4f system presented in figure 2 was configured using a different transparency with wide range of frequencies. The following exercises consisted in adding the four filters presented below in the frequency plane to verify their expected behavior qualitatively and quantitatively using an image of the transparency and the discrete approximation of equation 3 in Python.

1. Locating a variable-diameter iris diaphragm, 3 different lowpass filters were implemented, increasing the diameter of the iris diaphragm.

2. Using circular stops with diameters of 1, 0.5 and 0.25 mm at the frequency plane, 3 different high pass filters were configured, this time recording the output image.

3. Finally, to implement filtering operations in specific directions of the frequency plane, a variable slit was located both horizontally and vertically. In the same way, the behavior of both filters was verified by varying the size of the slit three times.

The setup of the 4f system with the variable-diameter iris diaphragm in the frequency plane can be seen in Fig. 5. In addition, the camera settings for all the recorded images are presented below in Table 1.

Table 1. Camera configurations.

Value	*System for viewing the FT*	*4F System*
Exposure time [ms]	0.95	1.00
Frame rate (FPS)	0.12	3.75

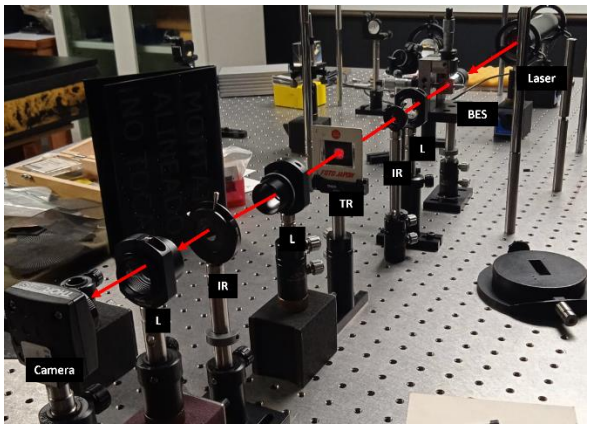

Fig. 5. 4F Setup. L, lens; IR, iris; TR, transparency; BES, beam expander system.

3. RESULTS

A. System for viewing the Fourier transform of an input transparency

In the ellipse transparency image [Fig. 6(a)] the experimental result of the frequency plane [Fig. 6(b)] has an orientation that is not seen in the theoretical one [Fig. 6(c)], this orientation can be possibly explained by the differences of the spot illumination and the hard alignment and non-uniformity of the spot. For the white band circle transparency in figure 6.d the theoretical cross and the bright and dark arcs are seen through *in silico* simulation, and they are also very similar with the cross seen in the experimental image [Fig. 6(e) and 6(f)). Finally, in the dark band circle transparency [fig. 6(g)], the general form of the theoretical and experimental image is conserved and some curved lines in the external part are both seen in the predicted and experimental images.

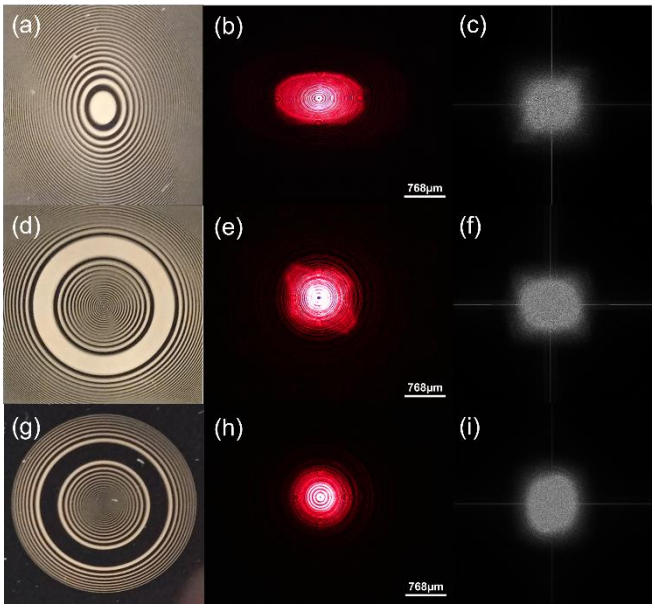

Fig. 6. Transparencies used to generate the Fourier transform plane, their experimental results, and their computed approximation, respectively: ellipse transparency (a), (b) and (c); white band circle transparency (d), (e) and (f); dark band circle transparency (g), (h) and (i).

The thin lines in the axis seen in theory results are not viewed experimentally possibly because they are too thin and because the theoretical still uses a cell camera to capture those images, and some fuzziness is seen in them.

In all the experimental images a pattern is seen, some clear circle +in the brightest area and a dark centered spot while there are none theoretically. These phenomena can be explained due to the way the camera takes the images, since it has a limited resolution and a limited exposure and sensibility, adjusted arbitrarily.

B. 4F System

The different filters applied can be seen in a digital way in Figure 7. These filters, from left to right and top to bottom, were increased in their values by a small percentage, simulating what was done experimentally.

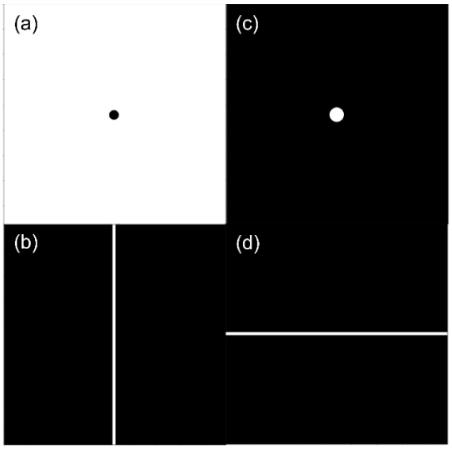

Fig. 7. Different filters applied in silico respectively: (a) spot filter; (c) iris filter; (b) vertical filter; (d) horizontal filter.

The multifrequency transparency experimental image and its comparison with the captured image of the transparency without filters is illustrated in Fig. 8.

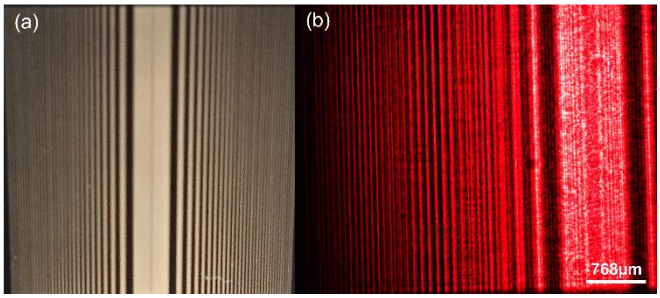

Figure 8. (a) Multifrequency transparency captured with a cell phone camera, and (b) its recorded image in the 4f system without any filter.

The simulated usages of the filters and their respective comparisons of the multifrequency transparency images can be seen in Figs. 9, 10, 11 and 12.

The different apertures of the iris and their experimental response are like the ones predicted by the Fourier code filtering seen in Fig. 9. Figs. 9(a) and 9(b) correspond to the largest iris aperture,

permitting high frequency pass, as we can see all the details in the extremes of the image. In Figs. 9(f) and 9(e) the image is blurred, as we can no longer see the details of the scene in the corners, as is also expected from the dwarfing of the iris inhibiting even lower frequencies to pass.

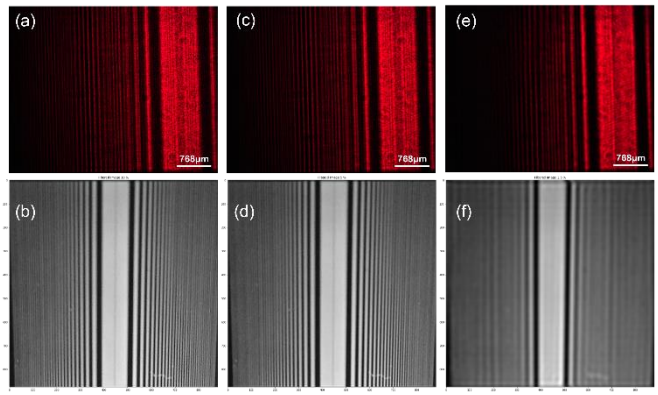

Fig. 9. Iris filter simulated and experimental applications respectively: (a) experimental big iris opening filter; (b) simulated big iris opening filter; (c) experimental medium iris opening filter; (d) simulated medium iris opening filter; (e) experimental low iris opening filter; (f) simulated low iris opening filter.

In Fig. 10 the stop filter was simulated and experimentally measured, with the smallest stop at the left in Figs. 10(a) and 10(b). Since this filter only blocks small and zero frequency signals, the details of the image can be seen in Figs. 10(a) and 10(b). As we increase the size of the spot, blocking even more higher frequencies almost all information is lost, as it can be illustrated in Figs. 10(e) and 10(f).

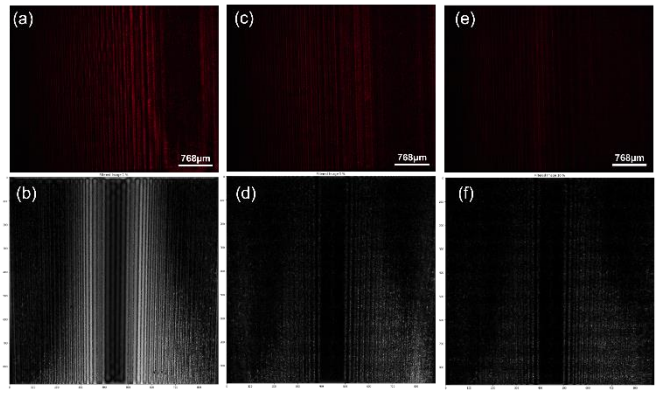

Fig 10. Simulated and experimental spot filter respectively: (a) experimental small spot filter; (b) simulated small spot filter; (c) experimental medium spot filter; (d) simulated medium spot filter; (e) experimental big spot filter; (f) simulated big spot filter.

In Fig. 11 the vertical filter was simulated and applied experimentally. In Figs. 11(a) and 11(b), a high width vertical aperture was applied, conserving all the signal attributes for the most part visually. As we move to the right of the figure, Figs. 11(e) and 11(f) the width decreases, making it harder to distinguish the image and blocking all horizontal frequencies, like most of them are in the image.

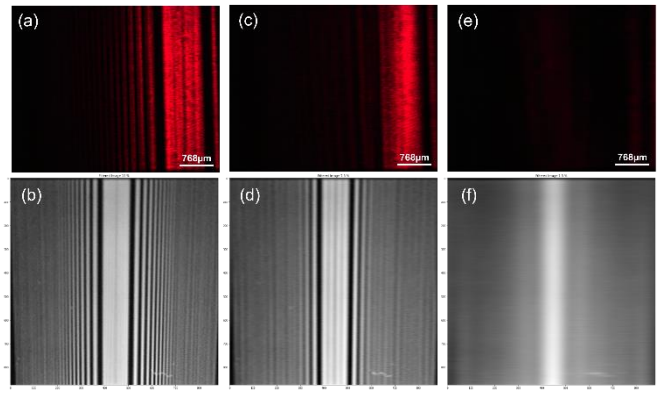

Fig 11. Simulated and experimental vertical filter respectively: (a) experimental big vertical aperture; (b) simulated big vertical aperture; (c) experimental medium vertical aperture; (d) simulated medium vertical aperture; (e) experimental small vertical aperture; (f) simulated small vertical aperture.

The simulated and experimental application of a horizontal slit are displayed in Fig. 2. In Figs. 12(a) and 12(b), the slit is wide both experimentally and simulated and all the characteristics of the images are preserved. As we see Figs. 12(e) and 12(f), the slit becomes thinner and less vertical frequencies pass through. In the simulated images on the thin slit, Figs. 12(e) and 12(f), details are sharper and information of blurriness or speckle noise in the original image are not seen in this one. The only and most notable difference between the simulated images and the real ones is the vertical diminishing of light, which is reduced as we make the slit thinner.

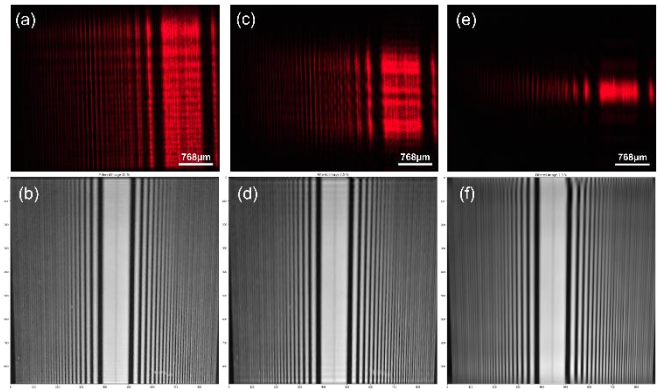

Fig 12. Simulated and experimental horizontal filter respectively: (a) experimental big horizontal aperture; (b) simulated big horizontal aperture; (c) experimental medium horizontal aperture; (d) simulated medium horizontal aperture; (e) experimental small horizontal aperture; (f) simulated small horizontal aperture.

4. CONCLUSIONS

The Fourier transformation of an image predicted by the formula and that which a lens produces are very similar. There are some differences in the final Fourier transformation attributed to the low resolution of the image taken to each transparency to calculate the transform.

Filtering in the Fourier spectrum reduces the signal in the frequency domain, with the center of it being the low frequencies and the high frequencies at higher radius which was verified showing that the low pass and high pass frequency filters work as expected from theory.

Disclosures. The authors declare no conflicts of interest.

Data availaility. Data underlying the results presented in this paper are not publicly available at this time but may be obtained from the authors upon reasonable request.

References

[1] C. Trujillo-Anaya, "Optical processing – 4F System," Universidad EAFIT, Medellín , 2021.

[2] Newport Corporation, "High-Energy Pinhole, Molybdenum, 10 µm, 900 Series," 2021. [Online]. Available: t.ly/Esub. [Accessed October 2021].

[3] Edmund Optics, "Olympus PLN 10X Objective," Edmund Optics Inc., 2021. [Online]. Available: t.ly/tCfh. [Accessed October 2021].

[4] Thorlabs, "AC254-200-A - f = 200 mm, Ø1" Achromatic Doublet, ARC: 400 - 700 nm," Thorlabs, Inc., 2021. [Online]. Available: t.ly/Ukb9. [Accessed October 2021].

[5] Thorlabs, "CMOS CAMERAS: USB 2.0 AND USB 3.0," Thorlabs, Inc., 12 August 2020. [Online]. Available: t.ly/qEK6. [Accessed October 2021].

[6] Thorlabs, "Broadband Halogen Fiber Optic Illuminators," 2020. [Online]. Available: t.ly/nA6E. [Accessed October 2021].

[7] Edmund Optics, "Olympus PLN 20X Objective," Edmund Optics Inc., 2021. [Online]. Available: t.ly/XKkg. [Accessed October 2021].